



Interaction of two-photon NOON state with ultrasonic wave

Piotr Kwiek^a

Institute of Experimental Physics, University of Gdańsk, Wita Stwosza 57, 80-952 Gdańsk, Poland

Received 17 December 2021 / Accepted 19 July 2022 / Published online 5 September 2022
© The Author(s) 2022

Abstract. The paper presents a classical and quantum description of the diffraction of two light beams incident on an ultrasonic wave at a positive and negative Bragg angle. The quantum description of the interaction with the ultrasonic wave was carried out for the two-photon NOON state. Study of diffraction of entangled pair of photon was performed in Mach–Zehnder interferometer wherein an output beam splitter is replaced by ultrasonic wave. It has been shown theoretically and experimentally that when a pair of photons generated from a parametric down-conversion was incident on two input ports of Mach–Zehnder interferometer with an acousto-optical beam splitter, then two-photon beats are observed at the output of the interferometer. The phenomenon of two-photon beats with the double frequency of the ultrasonic wave is the result of the Doppler effect on the ultrasonic wave. Time-correlated single-photon counting method was used to register the phenomenon of two-photon beats. The method of calibrating the interferometer with the use of an additional light source was presented in detail, which guarantees the observation of interaction of two-photon NOON state with ultrasonic wave.

1 Introduction

The first investigation on the interaction of a non-collinear correlated pair of photons generated from a parametric down-conversion with ultrasound wave was initiated by Zeillinger's group in 1995 [1]. The phenomenon of the interaction of collinear correlated photon pairs by an ultrasound wave in the Raman–Nath, Bragg and intermediate regions was investigated recently in 2015 [2, 3]. The experimental setup of the Zeillinger group resembles the Hong–Ou–Mandel interferometer [4] wherein an optical beam splitter is replaced by ultrasonic wave. In this case, the ultrasonic wave plays the role of an acousto-optical beam splitter, which can be classified as the so-called active beam splitters [5]. The authors of the above work in the theoretical description neglected the Doppler shift on the ultrasonic wave. So far, the experimental and theoretical results of the Zeillinger groups have not been verified by other researchers. In this situation, it is very important to determine when the influence of the Doppler shift should be taken into account in the interactions of entangled pairs of photons with the ultrasonic wave and when the Doppler effect can be neglected. The influence of the Doppler effect on interaction of two-photon NOON state with ultrasonic wave can be shown in a Mach–Zehnder interferometer,

in which the output beam splitter has been replaced by an ultrasonic wave.

Thirty years ago, Ou, Zou, Wang and Mandel [6] initiated fourth-order interference experiments in Mach–Zehnder interferometer. The above work shows theoretical and experimental confirmation that when two photons produced in the process of parametric down-conversion are incident simultaneously on the interferometer inputs then the probability of recording the photon coincidence between the outputs of the interferometer is proportional to the expression $(1 + \cos 2\theta)$, where θ is a relative phase shift between the interferometer arms. However, the number of single-photon counts at the interferometer outputs does not depend on the phase shift θ . So in this case we have fourth-order interference with 100 percent visibility, and we do not observe second-order interference. When one of the interferometer inputs is covered up and single photons is incident on the other input, it will occur second-order interference. Today we can say that in the experiment Ou, Zou, Wang and Mandel, the first beam splitter in the interferometer produced a two-photon NOON state, which at the input of the second beam splitter has the form $(|2\rangle_1|0\rangle_2 + \exp(2i\theta)|0\rangle_1|2\rangle_2)/\sqrt{2}$. So by replacing the second beam splitter in the Mach–Zehnder interferometer with an ultrasonic wave, we can investigate the interaction of two-photon NOON state with ultrasonic wave. When one of the interferometer inputs is covered up and single photons is incident on the other

^a e-mail: fizpk@ug.edu.pl (corresponding author)

input, it will occur second-order interference. Then, the recorded number of photons at the interferometer outputs will be proportional to the expression in the form $1 \pm \cos\theta$, where we have plus for one of the interferometer outputs and minus for the other output. In this case, at the input to the second beam splitter of the Mach–Zehnder interferometer, we have a single-photon state in the form $(|1\rangle_1|0\rangle_2 + \exp(i\theta)|0\rangle_1|1\rangle_2)/\sqrt{2}$ for which we observe second-order interference, i.e., classical interference effects.

In 1984, Leroy and Blomme [7] developed the diffraction theory of two coherent light beams incident on an ultrasonic wave at a positive and negative Bragg angle. As a result of the Doppler effect, the light diffracted on the ultrasonic wave is beaten with the frequency of the ultrasonic wave and the modulation of the light intensity in ± 1 -st diffraction order is proportional to the expression in the form $[1 \pm \cos(\Omega t + \theta)]$, where Ω is the angular frequency of ultrasonic wave. The above dependence is obtained for Raman–Nath parameter $v = \pi/2$, for which the ultrasonic wave becomes a 50:50 beam splitter.

The Leroy–Blomme theory was experimentally confirmed in 2019 and was completed with the initial phase of the ultrasonic wave [8]. The experimental setup in which the Leroy–Blomme theory was confirmed resembles the Mach–Zehnder interferometer [8] wherein an output beam splitter is replaced by ultrasonic wave. The above theory is necessary for the classical and quantum description of the operation of a Mach–Zehnder interferometer with an acousto-optical beam splitter.

It will be shown theoretically and experimentally that when two photons produced in the process of parametric down-conversion are incident in the same time on the input ports of the Mach–Zehnder interferometer with the acousto-optical beam splitter, the coincidence of photons between the outputs of the interferometer will change in time with the double frequency of the ultrasonic wave. The observed phenomenon is two-photon beats. It should be emphasized that the first attempt to register the two-photon beats phenomenon between two Michelson interferometers with acousto-optical beam splitters was made in 2003 [9]. Unfortunately, this effect was only recorded indirectly. Presented in this work two-photon beats measurements are direct and allow to record the modulation over time of the number of photon coincidence counts together with the modulation phase and the factors affecting it.

2 Mach–Zehnder interferometer with acousto-optical beam splitter

2.1 Classical description

Figure 1 shows a scheme of a Mach–Zehnder interferometer with an acousto-optical beam splitter. The

beam splitter (BS) at the input of the interferometer is a type of lossless 50:50 one, and at the output of the interferometer, the role of the beam splitter (AOBS) is performed by the ultrasonic wave. After passing through the beam splitter (BS), the monochromatic light wave E_0 is divided into two beams E_1 and E_2 , which are coherent with each other. The phase shifts of the reflected and transmitted beams depend on the construction of the beam splitter (BS). If the beam splitter is constructed as a single dielectric layer, the reflected and transmitted beams will differ in phase by a factor of $\exp(i\pi/2) = i$. The reflected light beams E_1 and E_2 from the (M_1) and (M_2) mirrors are incident symmetrically on the ultrasonic wave at the positive and negative Bragg angle β . There are only two orders of diffraction in the Bragg regime: 0-th and + 1-st or 0-th and –1-st depending on whether the angle of incidence is positive or negative [10].

The light beams E_1 and E_2 , passing through the ultrasonic wave, are diffracted thus creating diffraction orders. The direction of 0-th diffraction order originating from the E_1 beam coincides with the direction of + 1-st diffraction order originating from the E_2 beam, and the direction of 0-th order originating from the E_2 beam coincides with the direction of – 1-st order originating from the E_1 beam. The light which is diffracted to + 1-st diffraction order has an increased frequency by an ultrasonic frequency due to the Doppler effect, i.e., $\omega + \Omega$, whereas the light diffracted to – 1-st order has decreased frequency by an ultrasonic frequency $\omega - \Omega$. It should be stressed that in addition to the light of changed frequency in these diffraction orders there is light of unchanged frequency resulting from zero orders of E_1 and E_2 beams. The presence of light with a changed and unchanged frequency in a given diffraction order leads to a modulation of the light intensity in time due to the interference. This is the well-known phenomenon of beats.

The amplitudes of the diffracted light $\varphi_{1,0}$, $\varphi_{1,-1}$, $\varphi_{2,0}$ and $\varphi_{2,1}$ are required to calculate the light intensity modulation in the diffraction orders, where the first index indicates from which beam the given diffraction order comes from and the second index numbers the diffraction order. These amplitudes are obtained from solutions of Raman–Nath equations [11] modified by Mertens [12] who introduced the initial phase δ of the plane ultrasonic sinusoidal wave. As shown in [8], these amplitudes can be written in the following form:

$$\varphi_{1,0} = \cos(v/2) \quad (1a)$$

$$\varphi_{2,0} = \cos(v/2) \quad (1b)$$

$$\varphi_{1,-1} = -\sin(v/2)e^{i\delta} \quad (1c)$$

$$\varphi_{2,1} = \sin(v/2)e^{-i\delta} \quad (1d)$$

The amplitudes depend on the so-called Raman–Nath parameter, which is expressed by

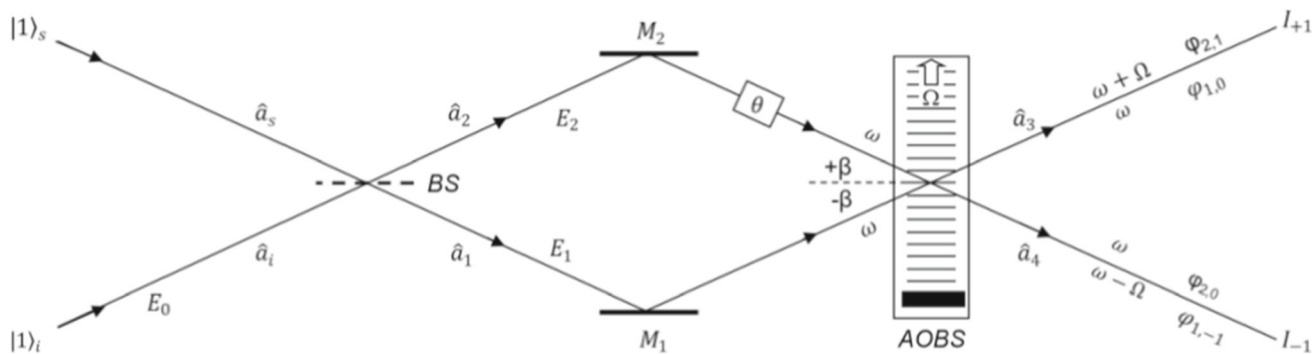


Fig. 1 Scheme of Mach–Zehnder interferometer with the acousto-optical beam splitter. E_0 , E_1 and E_2 are monochromatic light beams of angular frequency ω , β is Bragg angle, (BS) is lossless 50:50 beam splitter, AOBS is acousto-optical beam splitter, (M_1) and (M_2) are mirrors of 100% reflectivity, Ω -is the angular frequency of the ultrasonic wave, $\varphi_{1,0}$, $\varphi_{1,-1}$, $\varphi_{2,0}$, $\varphi_{2,1}$ are light amplitudes in the diffraction orders, and Θ is the phase shift between light beams

the formula:

$$v = \frac{2\pi\mu_1 L}{\lambda} \tag{2}$$

where μ_1 is the amplitude of changes in the refractive index caused by the ultrasonic wave, λ is the light wavelength, L is the width of the ultrasonic wave.

Using formulas (1a-1d), one may calculate the complex amplitude of light of ± 1 -st diffraction order as the sum of complex amplitudes coming from E_1 and E_2 beams as follows:

$$A_{+1} = A_0 e^{i\omega t} [i \cos(v/2) + \sin(v/2) e^{i\theta} e^{-i\delta} e^{i\Omega t}] \tag{3a}$$

$$A_{-1} = A_0 e^{i\omega t} [\cos(v/2) e^{i\theta} - i \sin(v/2) e^{i\delta} e^{-i\Omega t}] \tag{3b}$$

The angular frequency of incident light beams was denoted as ω , while θ as phase shift between light beams, and it was taken into account the fact that the beams E_1 and E_2 are shifted in phase by a factor $\exp(i\pi/2) = i$ that is caused by the beam splitter. More precisely, the reflected beam E_1 in the beam splitter is shifted in phase by $\pi/2$ in relation to the E_2 beam.

Assuming that the intensity of the incident light beams is equal and normalizing them to 0.5 which means that $A_0 A_0 = 0.5$, we can calculate, according to the formulas (3a, b), the intensity of light in ± 1 -st diffraction order as follows:

$$I_{+1} = A_{+1} A_{+1}^* = \frac{1}{2} [1 + \sin v \sin(\Omega t + \theta - \delta)] \tag{4a}$$

$$I_{-1} = A_{-1} A_{-1}^* = \frac{1}{2} [1 - \sin v \sin(\Omega t + \theta - \delta)] \tag{4b}$$

where $*$ means the complex conjugate.

From the above formulas, one can see that the intensity of light in ± 1 -st diffraction order is modulated

in time with the angular frequency Ω of the ultrasonic wave and the phase of modulation depends on the phase shift of the incident light waves θ and the initial phase of ultrasonic wave δ . In addition, the phase of modulation of light intensity in $+ 1$ -st diffraction order is always exactly 180 degrees shifted in relation to the phase of modulation of light intensity in the $- 1$ -st diffraction orders. According to the last formulas, the depth of modulation of light intensity in the diffraction orders reaches its first maximum (100 percent) for Raman–Nath parameter equal to $v = \pi/2$. The value of light intensity at the maximum modulation is twice as high as the intensity of light in each beam separately and is equal to their sum of intensities. The above conclusions resulting from formulas (4a) and (4b) were confirmed experimentally in 2019 [8].

For the value of the Raman–Nath parameter $v = \pi/2$ light amplitude in the diffraction orders according to the formulas (1a-1d), they will take the following form:

$$\varphi_{1,0} = \frac{1}{\sqrt{2}} \tag{5a}$$

$$\varphi_{2,0} = \frac{1}{\sqrt{2}} \tag{5b}$$

$$\varphi_{1,-1} = -\frac{1}{\sqrt{2}} e^{i\delta} \tag{5c}$$

$$\varphi_{2,1} = \frac{1}{\sqrt{2}} e^{-i\delta} \tag{5d}$$

Based on the above formulas, it can be concluded that the acousto-optical beam splitter for the value of the Raman–Nath parameter $v = \pi/2$ acts as 50:50 one.

2.2 Quantum description

Figure 1, which shows the scheme of the Mach–Zehnder interferometer with an acousto-optical beam splitter, shows photon annihilation operators at the input and output of the interferometer. They will be used for the quantum description of the interferometer. For a lossless 50:50 beam splitter (BS), assuming the reflected

beam suffers a $\pi/2$ phase shift, the output and input modes [13] are related according to

$$\hat{a}_1 = \frac{1}{\sqrt{2}}(\hat{a}_s + i\hat{a}_i) \tag{6a}$$

$$\hat{a}_2 = \frac{1}{\sqrt{2}}(\hat{a}_i + i\hat{a}_s) \tag{6b}$$

where \hat{a}_i and \hat{a}_s are the photon annihilation operators at the input of the beam splitter (BS), while \hat{a}_1 and \hat{a}_2 on its output.

The relations between the operators at the output and input of the acousto-optical beam splitter are much more complex than the relations (6a, b) for the beam splitter (BS) because it should be taken into the account the Doppler effect changing the frequency of photons which are diffracted to ± 1 -st diffraction order. As long as we only have photons of the same frequency in the interferometer, we may ignore the time dependence of the operators \hat{a} and \hat{a}^\dagger , where \hat{a}^\dagger denotes photon creation operator. The operator product $\hat{a}^\dagger\hat{a}$ does not depend on time, and hence, the time-dependent factor is omitted in cases where all photons have the same frequency. In the considered case, when the ultrasonic wave changes the frequency of the photons diffracted to ± 1 -st diffraction order, it cannot ignore the terms dependent on the frequency of the ultrasonic wave Ω . Taking into account that the angular frequency of the photons diffracted to $+ 1$ -st order is equal $\omega + \Omega$ and $\omega - \Omega$ for these diffracted to $- 1$ -st order and having also the amplitudes of light which passed through the acousto-optical beam splitter (AOBS) that are expressed by the formulas(1a,b,c,d) it can be obtained by the following relations between the output and input modes at the beam splitter.

$$\hat{a}_3 = \cos(v/2)\hat{a}_1 + \sin(v/2)e^{-i\delta}e^{i\theta}e^{i\Omega t}\hat{a}_2 \tag{7a}$$

$$\hat{a}_4 = \cos(v/2)e^{i\theta}\hat{a}_2 - \sin(v/2)e^{i\delta}e^{-i\Omega t}\hat{a}_1 \tag{7b}$$

where the angle θ represents a relative phase shift between the two paths in the interferometer.

When single photon is incident on one of the beam splitter inputs (BS) and there is vacuum only on the other input, then for the single-photon input state $|1\rangle_i|0\rangle_s$ the probabilities of photon detection in ± 1 -st diffraction order are as follows:

$${}_s\langle 0|_i\langle 1|\hat{a}_3^\dagger\hat{a}_3|1\rangle_i|0\rangle_s = \frac{1}{2}[1 + \sin v \sin(\Omega t + \theta - \delta)] \tag{8a}$$

$${}_s\langle 0|_i\langle 1|\hat{a}_4^\dagger\hat{a}_4|1\rangle_i|0\rangle_s = \frac{1}{2}[1 - \sin v \sin(\Omega t + \theta - \delta)] \tag{8b}$$

The formulas for the probabilities of detecting a photon in ± 1 -st diffraction order are the same as the formulas for the light intensity in ± 1 -st diffraction order

(4a, b) obtained for the classical description of the interferometer. Therefore, the conclusions resulting from formulas (8a, b) are the same as in the case of the classic description of the interferometer (4a, b).

When single photons are injected simultaneously into the two input ports of the 50:50 beam splitter (BS), then the incident state is $|1\rangle_i|1\rangle_s$ and the probability of detecting photons in $+ 1$ -st and $- 1$ -st diffraction orders is determined by the following formula:

$${}_s\langle 1|_i\langle 1|\hat{a}_3^\dagger\hat{a}_3|1\rangle_i|1\rangle_s = 1 = {}_s\langle 1|_i\langle 1|\hat{a}_4^\dagger\hat{a}_4|1\rangle_i|1\rangle_s \tag{9}$$

The last formula shows that the probability of detecting a photon in ± 1 -st diffraction order does not depend on time or phase shifts θ and δ .

While the probability of detecting coincidences of photons between $+ 1$ -st and $- 1$ -st diffraction orders is described by the formula (10). This formula describes the interaction of two-photon NOON state with ultrasonic wave.

$${}_s\langle 1|_i\langle 1|\hat{a}_3^\dagger\hat{a}_3\hat{a}_4^\dagger\hat{a}_4|1\rangle_i|1\rangle_s = \frac{1}{2}\sin^2 v[1 - \cos 2(\Omega t + \theta - \delta)] \tag{10}$$

It follows that the number of coincidence counts changes in time with twice the frequency of the ultrasonic wave as well as the dependence on phases θ and δ changes twice as fast as for the single-photon input state $|1\rangle_i|0\rangle_s$.

Moreover, the modulation depth is 100 percent regardless of the Raman–Nath parameter, whereas the modulation amplitude depends on the Raman–Nath parameter and reaches its first maximum for the Raman–Nath parameter $v = \pi/2$. For this parameter $v = \pi/2$ acousto-optical beam splitter acts like a 50:50 beam splitter as it was shown by the formulas (5a, b, c, d).

3 Experimental setup and its calibration

Figure 2 shows a scheme of the experimental setup developed for investigation of interaction of two-photon NOON state with ultrasonic wave together with a scheme of a system for calibrating the measuring system. The experimental setup consists of two lasers: one (405 nm) is used to generate photon pairs and the other (810 nm) to calibrate the measuring system. The wavelength of the light generated by the infrared laser (810 nm) is exactly equal to the wavelength of the photons produced by the photon pair source. Hence, when the acousto-optical light beam splitter is calibrated with an infrared laser (810 nm), it will also be calibrated for photon pairs.

A diode laser was used as a light source, generating a monochrome light wave with a wavelength of 810 nm and a power of 55 mW. The laser power was sufficient to be able to observe the laser beam with a night vision device, which greatly facilitates the adjustment of the

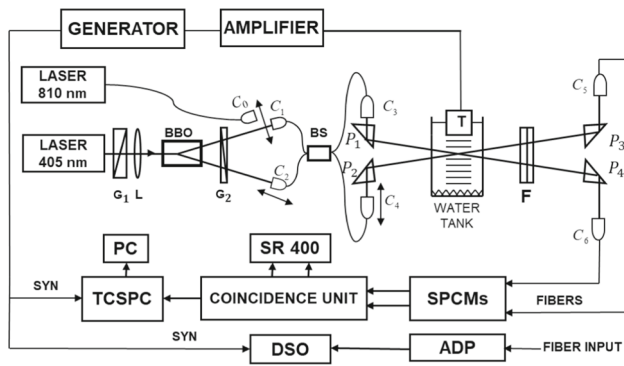


Fig. 2 Scheme of the experimental setup. Major components include red and violet laser (810 nm and 405 nm), down-conversion crystal (BBO), Glan–Taylor polarizers (G_1 , G_2), lens (L), fiber optic beam splitter (BS), collimators (C_0 – C_6), right-angle prisms (P_1 – P_4), optical filters set (F) (long-pass and band-pass filter), water tank with an ultrasonic transducer (T), single-photon counting modules (SPCMs), coincidence unit, dual-channel photon counter (SR 400), time-correlated single-photon counting board (TCSPC) with computer (PC), avalanche photo diode with an amplifier (APD), digital storage oscilloscope (DSO)

measuring system. A beam of light from the laser was directed through an optical fiber and collimators (C_0) and (C_1) to a fiber optic beam splitter (BS), which divided the beam into two beams of the same intensity. The collimator (C_0) was placed on the translating stage ensuring precise movement perpendicularly to its optical axis, giving the possibility to choose light from the infrared laser or photons from the source of photon pairs. The output optical fibers from the beam splitter (BS) were ended with collimators of light (C_3) and (C_4) that allowed for obtaining parallel light beams with a diameter of 3 mm. The fiber optic beam splitter was made of single-mode polarization maintaining fibers, which ensured a homogeneous distribution of the intensity of light coming from the collimators and constant direction of light polarization. So formed beams were directed by a prisms (P_1) and (P_2) and they were incident exactly at Bragg angle on a progressive ultrasonic wave propagating in a water tank. The ultrasonic wave was generated using circular LiNbO₃ transducer (T) with the fundamental frequency of 10.79 MHz, 22.4 mm in diameter, with coaxial electrodes excited at a frequency of 32.370 MHz, which corresponds to the third harmonic. Standing waves in the water tank were avoided by a careful selection of a suitable absorbing material.

Light diffracted by the ultrasonic wave was directed by means of prisms (P_3) and (P_4) toward collimators, which in turn directed it to single-mode optical fibers using collimators (C_5) and (C_6). Light from optical fibers was measured using an avalanche photo diode (APD) with an amplifier and recorded using a digital storage oscilloscope (DSO).

The oscilloscope and the amplifier supplying the ultrasonic transducer (T) were controlled from the

same generator, which ensured a constant phase shift between electrical signal supplying ultrasonic transducer and electrical pulses, which synchronize the oscilloscope time base. By controlling the depth of light intensity modulation on the oscilloscope, we can precisely set the Bragg angles and the Raman–Nath parameter.

After precise determination of the Bragg angles and the Raman–Nath parameter $v = \pi/2$, the laser power (810 nm) was reduced below the threshold value. Then, the spectrum of laser light became very wide. After passing through the filters set (F), the light had a wavelength of 810 nm and a spectral width of 10 nm, i.e., the same wavelength and spectral width as photon pairs. The light coherence path for this spectral width is only 65 μm . By examining the depth of light intensity modulation depending on the optical paths difference of the light beams reaching the ultrasonic wave, we can control the optical paths difference. For zero difference in optical paths, we get the maximum depth of light intensity modulation. For this, (C_4) collimator was used, which was placed on a translation stage with piezo-elements providing rough and precise movement along its optical axis. This solution allowed for precise adjustment of optical paths of light beams reaching the ultrasonic wave and changing the phase shift θ between them.

Figure 3 shows the modulation of the intensity of light in + 1-st diffraction order registered on the (DSO) oscilloscope for the Raman–Nath parameter equal $v = \pi/2$ and light with a spectral width of 10 nm. The modulation depth for this parameter assumes the maximum value, and it is 100 percent according to formula (4a). The modulation of the light intensity in + 1-st diffraction order shown in Fig. 3 was normalized to the intensity of light passing through the water tank in the absence of ultrasonic wave. On the other hand, the signal value measured with the oscilloscope when the laser was turned off was assumed to be zero.

The normalization procedure allowed to compare the measured modulation of light intensity with the theoretical curve obtained basing on the formula (4a) whose phase was numerically matched to the phase of the experimental curve. It can be noticed in Fig. 3 that the measured modulation depth of light intensity (often called visibility in quantum optics) reaches 93 percent, which is very close to the theoretical value of 100 percent for monochromatic light beams.

So good agreement of light intensity modulation of spectral width of 10 nm and theoretical curve for monochromatic light will ensure that optical paths are equal, so that it allows to go to the next stage of the calibration of the interferometer.

It can easily be seen that the Mach–Zehnder interferometer with the acousto-optical beam splitter after turning off of the ultrasonic wave and turning on the source of photons pairs becomes Hong–Ou–Mandel interferometer, whose operation is shown below.

Light from an InGaN laser diode (405 nm) is sent through a (BBO) crystal producing photon pairs via type-I parametric down-conversion [13]. The (BBO) crystal was positioned exactly in the laser beam waist

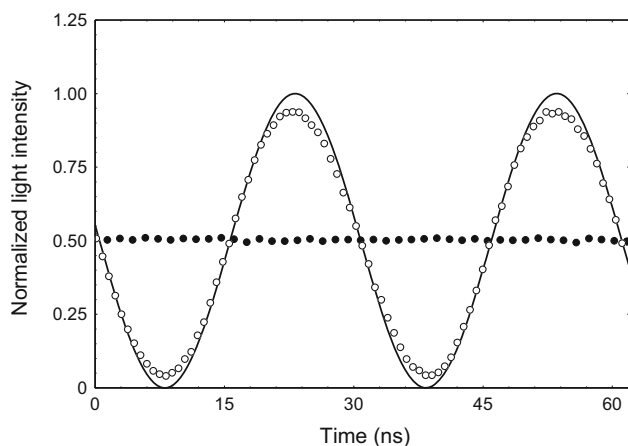


Fig. 3 Temporal modulation of light intensity in + 1-st diffraction order for Raman–Nath parameter. $v = \pi/2$. According to the formula (4a), theoretical prediction is drawn by solid line and experimental data as hollow symbols. The light intensity with the absence of an ultrasonic wave is denoted by filled symbols. Time axis covers two ultrasonic wave periods

associated with the lens (L). The crystal was oriented for non-collinear down-conversion of the pairs with equal wavelengths (810 nm). The crystal was placed between two crossed polarizers (G_1) and (G_2). The first polarizer (G_1) ensures that pump photons are linearly polarized and retain an appropriate polarization direction with respect to the optical axis of the (BBO) crystal. The second polarizer (G_2) eliminates the pump beam, which has polarization orthogonal to that of down-converted photons. The photon pairs after passing through the beam splitter and the set of two filters (F) were directed by single-mode optical fibers to single-photon counting modules (SPCMs).

For better separation from the pump laser photons, a supplementary long-pass filter (RG780) is introduced, which passes wavelengths longer than 780 nm, while the aim of the band-pass filter is to pass further only the photons of 810 nm wavelength with 10 nm bandwidth (FWHM). In Fig. 2, the set of these two filters is marked with the letter (F). Electrical signals from the (SPCMs), after passing through a coincidence unit with coincidence window of 22 ns, were registered by a dual-channel photon counter (SR 400). Further adjustment of the measuring system comes down to finding the Hong–Ou–Mandel dip. For this, a (C_2) collimator was used, which was placed on a translation stage providing precise movement along its optical axis. Figure 4 shows the Hong–Ou–Mandel effect when changing the optical path difference by moving the (C_2) collimator along the optical path. The number of coincidence counts does not go exactly to zero as shown in the theoretical curve in Fig. 4. In practice, it is close to zero, but not exactly zero. The number of coincidence counts will drop to zero when the identical input photons overlap perfectly in time.

Calibration of the Mach–Zehnder interferometer with an acousto-optical light beam splitter is ended with

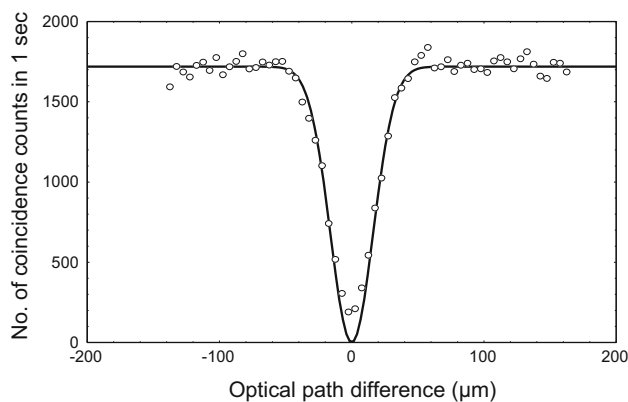


Fig. 4 Hong–Ou–Mandel effect [4]. The theoretical curve is drawn with a solid line and the experimental data as hollow symbols. The visibility of the Hong–Ou–Mandel dip is 89%

setting the (C_2) collimator in a position for which there is a minimum coincidence of photon pairs.

As shown in the theoretical part, at the output of the Mach–Zehnder interferometer with an acousto-optical beam splitter, the number of photons varies in time with the frequency of the ultrasonic wave (8a, b) or the number of photon coincidence between interferometer outputs will change in time with the double frequency of the ultrasonic wave (10).

Changes in the number of photons or the number of their coincidences were recorded using time-correlated single-photon counting (TCSPC) method. This method is mainly used for fluorescence decay measurements with picoseconds time resolution [14], but also it perfectly suits for recording periodic time changes in the number of photons. Pico Quant PC-board model Time Harp 100 for time-correlated single-photon counting was used for the measurements. The PC-board and the amplifier supplying the ultrasonic transducer (T) were controlled from the same generator, which ensured a constant phase shift between electrical signal supplying ultrasonic transducer and electrical pulses which synchronize the TCSPC electronics.

4 Experimental results

At first, the results of the time modulation of the number of single-photon counts at the output of the interferometer will be presented when single photons incident to one of the beam splitter inputs (BS). For the single-photon input state $|1\rangle_i|0\rangle_s$, the probabilities of photon detection in + 1-st diffraction order (i.e., at the output of the interferometer) are expressed by the formula (8a). The number of registered single photons in + 1-st diffraction order as a function of time is shown in Fig. 5. Single-photon counts were measured using the TCSPC method with 640 ps time resolution. PC-board for time-correlated single-photon counting was synchronized with every second pulse from the generator driving the ultrasonic transducer. The

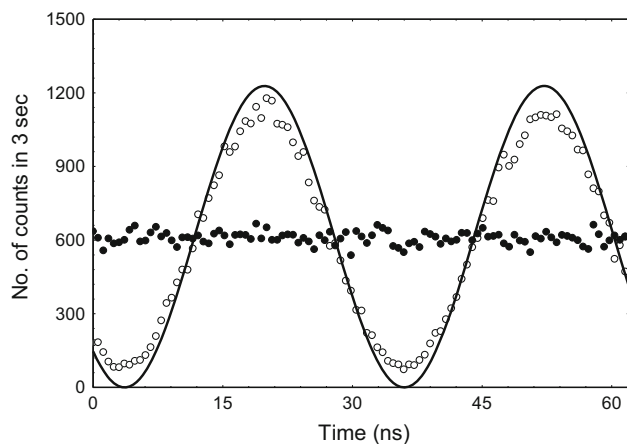


Fig. 5 Modulation in time of number of counts in +1-st diffraction order for Raman–Nath parameter $v = \pi/2$. Time axis covers two periods of ultrasonic wave. According to the formula (8a), theoretical prediction is drawn by solid line and experimental data as hollow symbols. The number of counts with the absence of an ultrasonic wave is denoted by filled symbols

control of every second pulse caused that the time axis on the diagram included two periods of ultrasonic wave (≈ 62 ns).

As was pointed out earlier when single photons incident on one of the beam splitter inputs (BS), then the formulas for probabilities of detecting a photon in ± 1 -st diffraction order (8a, b) are the same as the formulas for the light intensity in ± 1 -st diffraction order (4a, b) obtained for the classical description of the interferometer, whereas the modulation frequencies in the both cases (classical and quantum) are equal to the frequency of the ultrasonic wave. Comparing the results of modulation in time of the light intensity at the output of the interferometer when it is illuminated by a light wave beam (Fig. 3) with the results when there are single photons at the input (Fig. 5), it can be seen that the modulation depths are almost identical. The modulation depth for single photons is about 90 percent and for the light wave beam about 93 percent, while the theoretical modulation depth is 100 percent for the Raman–Nath parameter $v = \pi/2$ for which both measurements were taken. It can be easily seen that the results for single photons show greater fluctuations than the results for the light wave beam. This is mainly due to the low number of single-photon counts. According to the Poisson statistics, the uncertainty σ in the number of photons counts is given by $\sigma = \sqrt{N}$, where N is the number of photon counts. For longer measurement times, a greater number of single-photon counts will be obtained, but at the same time it will increase the influence of θ and δ phase fluctuations which next will reduce the modulation depth, while the phase fluctuations in the electronics were much smaller than the fluctuations of phases θ and δ and had practically no effect on the fluctuation of the modulation phase.

When two single photons are injected simultaneously into the two inputs of the interferometer, then the

coincidence of photons between the outputs of the interferometer, i.e., between +1-st and –1-st diffraction order, can be registered. The number of photon coincidences, shown in Fig. 6a, at the output of the interferometer changes periodically in time with a frequency twice the frequency of the ultrasonic wave and the modulation depth close to 100 percent. The obtained coincidence result is in agreement with the formula (10), describing the interaction of two-photon NOON state with ultrasonic wave, as a result of which we are observing the phenomenon of two-photon beats. Figure 6b shows the number of single-photon counts in +1-st diffraction order, i.e., at the output of the interferometer. According to formula (9), the number of single-photon count at the output of the interferometer should not depend on time. The slight modulation with the frequency of the ultrasonic wave of the number of single-photon counts in Fig. 6b is due to the small difference in the number of photons at the inputs of the interferometer.

5 Conclusions

The aim of this work was to investigate interaction of two-photon NOON state with ultrasonic wave. The twin single-photon states at the input of a 50:50 beam splitter of Mach–Zehnder interferometer are sufficient to generate the two-photon NOON state inside interferometer.

By replacing the output beam splitter of the Mach–Zehnder interferometer with an acousto-optical beam splitter, it was possible to investigate the interaction of single photon in the form $(|1\rangle_1|0\rangle_2 + \exp(i\theta)|0\rangle_1|1\rangle_2)/\sqrt{2}$ and two-photon NOON state $(|2\rangle_1|0\rangle_2 + \exp(2i\theta)|0\rangle_1|2\rangle_2)/\sqrt{2}$ with ultrasonic wave.

For the first case (8a, b), the photon beats with ultrasonic frequency are observed at the outputs of acousto-optical beam splitter. The modulation depth is a function of the Raman–Nath parameter and varies from 0 to 100 percent for a parameter change from $v = 0$ to $v = \pi/2$, while modulation phase depends on θ and δ .

In the second case (10), two-photon beats between the outputs of the acousto-optical beam splitter are observed with twice the frequency of the ultrasonic wave. Also, the modulation phase depends on the double value of θ and δ . The modulation depth is 100 percent and does not depend on the Raman–Nath parameter as it was in the previous case.

The theoretical predictions were confirmed experimentally and the time-correlated single-photon counting method appeared to be an excellent method of studying changes in time the number of photon counts or coincidences.

When in the Mach–Zehnder interferometer the output beam splitter is replaced with an acousto-optical light splitter, the interferometer becomes a heterodyne Mach–Zehnder interferometer, despite the fact that the frequencies of the photons in the arms of the

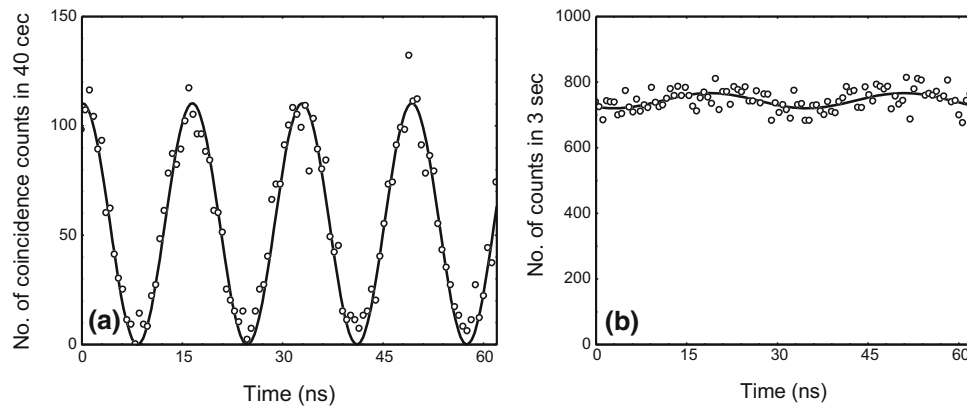


Fig. 6 **a** Two-photon beats. Theoretical prediction according to the formula (10) is drawn by solid line and experimental data as hollow symbols. **b** Modulation in time of number of counts in +1-st diffraction order. The experimental results are denoted as hollow symbols and the continuous line is the curve modulated with the frequency of the ultrasonic wave best suited to the experimental results. The time axis covers two ultrasonic wave periods and the presented results, both **a** and **b** are obtained for Raman–Nath parameter equal to $v = \pi/2$

interferometer are the same. This greatly simplifies the construction of the heterodyne Mach–Zehnder interferometer [15].

It is worth emphasizing, what was mentioned earlier, that the Mach–Zehnder interferometer with an acousto-optical beam splitter becomes the Hong–Ou–Mandel interferometer after switching off the ultrasonic wave. This allows to quickly check if interferometer is correctly adjust on Hong–Ou–Mandel dip.

The dependence of the modulation phase of the number of photons or coincidences either on the phase shift θ between the arms of the interferometer or the initial phase δ of the ultrasonic wave will create very wide range possibilities of interferometric measurements [16, 17].

Acknowledgements I wish to express my gratitude to Professors P. Bojarski and J. Kwela for support during the implementation of this work. I am also grateful to Doctor A. Markiewicz for her help in the final preparation of this paper.

Data Availability Statement This manuscript has no associated data or the data will not be deposited. [Authors' comment: I do not provide data. The experimental results are shown in the paper.]

Open Access This article is licensed under a Creative Commons Attribution 4.0 International License, which permits use, sharing, adaptation, distribution and reproduction in any medium or format, as long as you give appropriate credit to the original author(s) and the source, provide a link to the Creative Commons licence, and indicate if changes were made. The images or other third party material in this article are included in the article's Creative Commons licence, unless indicated otherwise in a credit line to the material. If material is not included in the article's Creative Commons licence and your intended use is not permitted by statutory regulation or exceeds the permitted use, you will need to

obtain permission directly from the copyright holder. To view a copy of this licence, visit <http://creativecommons.org/licenses/by/4.0/>.

References

1. B. Dopfer, P.G. Kwiat, H. Weinfurter, A. Zeilinger, M.A. Horne, *Phys. Rev. A* **52**, R2531 (1995)
2. P. Kwiek, *Ultrasonics* **57**, 153 (2015)
3. P. Kwiek, *Appl. Opt.* **54**, 5662 (2015)
4. C.K. Hong, Z.Y. Ou, L. Mandel, *Phys. Rev. Lett.* **59**, 2044 (1987)
5. M.G. Raymer, S.J. van Enk, C.J. McKinstrie, H.J. McGuinness, *Opt. Commun.* **283**, 747 (2010)
6. Z.Y. Ou, X.Y. Zou, L.J. Wang, L. Mandel, *Phys. Rev. A* **42**, 2957 (1990)
7. O. Leroy, E. Blomme, *Ultrasonics* **22**, 125 (1984)
8. P. Kwiek, *Proc. SPIE* **11210**, 1121005 (2019)
9. A. Stefanov, H. Zbiden, N. Gisin, A. Suarez, *Phys. Rev. A* **67**, 042115 (2003)
10. P. Phariseau, *Proc. Indian Acad. Sci.* **44**, 165 (1956)
11. N. S. Nagendra Nath, *Proc. Indian Acad. Sci.* **4**, 222 (1936)
12. R. Mertens, *Proc. Indian Acad. Sci.* **50**, 289 (1959)
13. C. C. Gerry, P. L. Knight, *Introductory Quantum Optics* (Cambridge University Press, 2005)
14. D.V.O. O'Connor, D. Phillips, *Time-correlated single Photon counting* (Academic Press, London, 1984)
15. V. Wand, J. Bogenstahl, C. Braxmaier, K. Danzmann, A. García, F. Guzmán, G. Heinzl, J. Hough, O. Jenrich, C. Killow, D. Robertson, Z. Sodnik, F. Steier, H. Ward, *Class. Quantum Grav.* **23**, S159 (2006)
16. M. Eaton, R. Nehra, A. Win, O. Pfister, *Phys. Rev. A* **103**, 013726 (2021)
17. W. Zhong, L. Zhou, Y.-B. Sheng, *Phys. Rev. A* **103**, 042611 (2021)